Skin friction under pressure. The role of micromechanics

Surface Topography: Metrology and Properties

OPEN ACCESS

PAPER

Skin friction under pressure. The role of micromechanics

Maria F Leyva-Mendivil[1,2], Jakub Lengiewicz[3] and Georges Limbert[1,2,4]

[1] Faculty of Engineering and the Environment, National Centre for Advanced Tribology at Southampton (nCATS), University of Southampton, Southampton SO17 1BJ, United Kingdom
[2] Faculty of Engineering and the Environment, Bioengineering Research Group, University of Southampton, Southampton SO17 1BJ, United Kingdom
[3] Institute of Fundamental Technological Research, Polish Academy of Sciences (IPPT PAN), ul. Pawinskiego 5B, 02-106 Warsaw, Poland
[4] Faculty of Health Sciences, Laboratory of Biomechanics and Mechanobiology, Department of Human Biology, Division of Biomedical Engineering, University of Cape Town, Observatory 7935, South Africa

E-mail: g.limbert@soton.ac.uk

Keywords: skin friction, contact mechanics, pressure, microstructure, finite element, homogenisation, material properties

RECEIVED
19 October 2017

REVISED
13 December 2017

ACCEPTED FOR PUBLICATION
19 December 2017

PUBLISHED
19 January 2018

Abstract

The role of contact pressure on skin friction has been documented in multiple experimental studies. Skin friction significantly raises in the low-pressure regime as load increases while, after a critical pressure value is reached, the coefficient of friction of skin against an external surface becomes mostly insensitive to contact pressure. However, up to now, no study has elucidated the qualitative and quantitative nature of the interplay between contact pressure, the material and microstructural properties of the skin, the size of an indenting slider and the resulting measured macroscopic coefficient of friction. A mechanistic understanding of these aspects is essential for guiding the rational design of products intended to interact with the skin through optimally-tuned surface and/or microstructural properties.

Here, an anatomically-realistic 2D multi-layer finite element model of the skin was embedded within a computational contact homogenisation procedure. The main objective was to investigate the sensitivity of macroscopic skin friction to the parameters discussed above, in addition to the local (i.e. microscopic) coefficient of friction defined at skin asperity level. This was accomplished via the design of a large-scale computational experiment featuring 312 analyses. Results confirmed the potentially major role of finite deformations of skin asperities on the resulting macroscopic friction. This effect was shown to be modulated by the level of contact pressure and relative size of skin surface asperities compared to those of a rigid slider. The numerical study also corroborated experimental observations concerning the existence of two contact pressure regimes where macroscopic friction steeply and non-linearly increases up to a critical value, and then remains approximately constant as pressure increases further.

The proposed computational modelling platform offers attractive features which are beyond the reach of current analytical models of skin friction, namely, the ability to accommodate arbitrary kinematics, non-linear constitutive properties and the complex skin microstructure.

1. Introduction

In the last decade, biotribology has emerged as a fast-growing area of research focused on understanding the contact and surface interactions of biological tissues with natural and engineered surfaces. Although skin tribology encompasses many branches of soft matter physics and biology, and therefore is a very broad research arena, considerable efforts are currently devoted to specifically develop theories, experiments and models to describe and explain skin friction. This interest in academia and industry stems from the fact that she skin covers the entirety of the human body, and therefore is our primary and largest interface to the external environment. In their daily life humans physically interact with their outside world through their skin. These interactions range from contact with bedding surfaces, clothes, prosthetic liners and shoes, through personal care products including razors and lotions, to electronic surfaces featuring tactile display

and vehicle interiors [1]. Little imagination is required to appreciate how much skin tribology is intimately linked to human life and activities.

Skin friction is a highly non-linear multi-factorial phenomenon featuring complex multiphysics and multiscale feedback mechanisms [2–7]. This extreme complexity renders the experimental characterisation and modelling of skin friction particularly challenging. To date, no unified theory encompassing these phenomena is available, and this hinders our ability to, first understand mechanistically the basic mechanisms involved, and second, to develop physics-based predictive tools to assist engineers in the design of product intended to interact with the skin. The underlying aim is to enable the rational design of improved and innovative products that optimally interact with the skin through finely tuned engineered surface characteristics. A wide range of such industrial products can actually cause discomfort to the user, and, in some cases, irritation and even damage to the skin. Examples include personal care goods such as nappies and incontinence products, facial cleansing and shaving devices, electronic wearables and limb prostheses. Whilst this affects products aimed at users of all ages, the problem is exacerbated for older users, as ageing skin progressively loses elasticity and resilience whilst becoming more fragile and susceptible to shear damage [8]. There is a direct relationship between the shear stress acting on the skin and the development of skin injuries, but the exact mechanics of soft contact, deformation-induced and adhesion-induced skin friction, as well as shear load transmission, remains unclear and requires further research [3].

An interesting aspect of skin friction is that it simultaneously conditions load transmission through the skin surface whilst also being a by-product of it. Cross-talk mechanisms associated with deformation and stress are therefore at the heart of skin friction [2–4]. In their excellent review and analysis paper, Derler and Gerhardt [2] conclude that skin friction depends on loading conditions (pressure and sliding velocity) and material/structural properties of skin and contacting surface (surface roughness, mechanical, chemical and other physical properties).

The dependence of skin friction to either normal load or pressure has been widely documented. As far as 1983, in an experimental study, Wolfram [7] observed that the skin's coefficient of friction is relatively insensitive to large loads, but highly sensitive to lower loads. The influence of sliding velocity on the friction response of skin is related to its viscoelastic properties. These characteristics are also present in soft elastic solids including rubbers, for which friction theories and computational formulations have been widely developed [9–14]. Borrowing from some of these ideas, Adams *et al* [15] described skin friction as a mechanism involving the contribution of distinct hysteresis and adhesion components. The hysteresis component is related to energy loss during viscoelastic recovery (spring back of the material after being deformed by the contacting surface). In frictionless conditions, the slower recovery of a surface disturbs the distribution of forces at the contact interface resulting in a force opposing the sliding motion. In this case, the deformation is proportional to the pressure at the contact interface and, because the recovery of the material is a time dependent property, sliding velocity has a direct effect on the distribution of forces at the contact area, thus affecting the overall skin friction behaviour. The adhesion component is related to the real area of contact whereby the distance between the contacting surfaces is small enough for atomic interaction forces to contribute to the resistance to motion [16].

Because the friction of skin is intimately conditioned by, among other types of physical process [17], its micromechanics during contact interactions, any alterations of material and microstructural properties will alter its frictional behaviour. The *stratum corneum* which is the outermost layer of the skin is particularly sensitive to environmental conditions, notably, relative humidity [18, 19]. Moisture can be absorbed into the *stratum corneum*, resulting in swelling of corneocytes, thickness increase [20], significant reduction in Young's modulus [18], Poisson's ratio increase [21] and changes in the adhesion properties of the skin surface [22]. Besides its potentially major contribution to the overall mechanics of skin [3, 4, 23–25], the *stratum corneum* layer can stiffen by up to three orders of magnitude, in a matter of hours, when relative humidity levels drop from 100 to 0% [18, 19, 26, 27]. Simultaneous increase in hydration and temperature levels amplify fluctuations of skin friction [28, 29] and also reduce the resistance to delamination of the *stratum corneum* [18].

These physical effects are encapsulated by the notion of *skin microclimate*, whose role in the aetiology and evolution of pressure ulcers is being increasingly recognised [30, 31].

Anatomically-based modelling of the skin [1, 25] offers the promise of deconstructing the complexity of its biophysical and tribological behaviour by enabling fully-controlled parametric analyses whilst also accounting for key microstructural features of the skin. Recently, such an approach was used to study skin friction, in combination with a multiscale computational homogenisation procedure [3, 4]. Plane-strain finite element modelling was used to simulate finite sliding of a sub-millimetric indenter (three sizes were considered) over a geometrically realistic skin surface as well as internal microstructure, including the *stratum corneum*, viable epidermis and dermis layers. For the local contact problem, at the scale of skin asperities, a variable *local* coefficient of friction was assigned between the indenter and the skin surface. From the reaction force of the indenter that was measured at each position of the sliding path, a *global* or *macroscopic* coefficient of friction was inferred [4, 32]. In their first skin friction study, Leyva-Mendivil *et al* [4] highlighted

the significant role that skin surface topography and internal microstructure can have in modulating and increasing the deformation component of macroscopic friction. Stiffening of the *stratum corneum* was also shown to provide a structural mechanism by which friction increases. The same approach was later used by Leyva-Mendivil *et al* [3] to investigate how the micromechanics of multi-asperity contact conditions shear load transmission across skin layers.

In both these studies the influence of normal load or pressure on macroscopic friction was not systematically investigated. As discussed earlier, experimental evidence suggest that contact pressure is a key variable controlling the nature and magnitude of macroscopic friction [2, 7]. Motivated by this gap in knowledge, the objective of the study presented in this paper is to systematically analyse the influence of pressure, as well as that of indenter size and material properties of the *stratum corneum*, on macroscopic friction. This is achieved by using the same proven computational friction homogenisation approach of our earlier studies [3, 4]. The manuscript is organised as follows. The general modelling methodology and design of computational experiment are detailed in section 2 while numerical results are presented in section 3 and discussed in the following section. Finally, conclusions to the study are drawn in section 5.

2. Modelling methodology

In this research, we followed the experimentally-based computational methodology adopted in a previous study aiming to characterise the influence of skin microstructure on its macroscopic frictional response [4]. The basic approach is briefly described here for sake of completeness. It consists of *implicitly* simulating contact of a macroscopically flat skin sliding against a macroscopically flat counteracting rigid surface through a non-linear finite element contact homogenisation procedure. Both of these macroscopically flat surfaces contain micro-asperities which contribute to their relative sliding resistance through the interlocking of the asperities' geometry and the local (i.e. microscopic) adhesion and deformation interactions (figure 1). The computational procedure effectively integrates microscopic scale interactions between skin asperities and those of the rigid surface. However, it was assumed that rigid asperities were placed sufficiently apart from each other to eliminate potential mutual mechanical interference so that only one single rigid asperity could be considered in the numerical homogenisation procedure. The modelling was casted into a two-dimensional (2D) plane-strain framework. The main assumption of this work was that the *microscopically rough* rigid surface was made of randomly positioned identical cylindrical indenters. Based on the assumptions described above, a representative microscopic sample consisting of a skin sample in contact with a single rigid indenter can be used to derive the global (i.e. macroscopic) friction response of the macroscopically flat surfaces. More details can be found in Leyva-Mendivil *et al* [4].

Here, the main novel contribution lays in the characterisation of the simultaneous sensitivity of macroscopic friction to contact pressure and indenter size. Details of the computational homogenisation procedure, modelling of the skin and design of computational experiments are provided below.

2.1. Computational homogenisation procedure

The homogenisation of microscopic sliding contact interactions [4, 32] is based on the existence of a representative microscopic region, henceforth referred as microscopic sample or micro-sample (figure 1). Both surfaces of the skin and contacting material are assumed to be representative of the full surface topographic characteristics, along the total (macroscopic) length of the contacting surface L_C. The contacting surface is represented as a regular periodic surface with asperities of equal sizes, separated by a distance λ (also referred as wavelength). The micro-sample length L contains the representative surface of skin. For this study, it is assumed that $\lambda \gg L$ to ensure that the interference between each asperity-skin contact is negligible.

As introduced in Leyva-Mendivil *et al* [4], under certain assumptions (as described in the introduction part of section 2—Modelling methodology of the present paper), the frictional response of the macroscopic nominally flat surfaces (*global* friction) can be retrieved using a special homogenisation procedure only done for a single micro-sample. The procedure relies on computing the average traction vector as an integral from local tractions of the indenter sliding over the skin micro-sample. In a discrete setting, this consists in taking measurements of the normal and tangential components of the traction vector $\boldsymbol{f}^i = f_T^i \mathbf{e}_x + f_N^i \mathbf{e}_y$ at each position x^i during sliding over the total micro-sample length L, where $\{\mathbf{e}_x, \mathbf{e}_y\}$ are the referential basis unit vectors. The normal and tangential components of the average traction vector $\bar{f}_N$ and $\bar{f}_T$ are then calculated as:

$$\bar{f}_N \simeq \frac{1}{L} \sum_i \frac{1}{2} \left(f_N^i + f_N^{i-1} \right) \left(x^i - x^{i-1} \right) \qquad (1)$$

$$\bar{f}_T \simeq \frac{1}{L} \sum_i \frac{1}{2} \left(f_T^i + f_T^{i-1} \right) \left(x^i - x^{i-1} \right). \qquad (2)$$

The traction vector of the macroscopic surface (F_N, F_T) is obtained by multiplying equations (1) and (2) by the asperity density $\rho_a = 1/\lambda$ (number of asperities per unit length) and the total length L_C of the contacting surface as:

$$F_N = \bar{f}_N \rho_a L_C, \quad F_T = \bar{f}_T \rho_a L_C. \qquad (3)$$

So, the global or macroscopic coefficient of friction is given by:

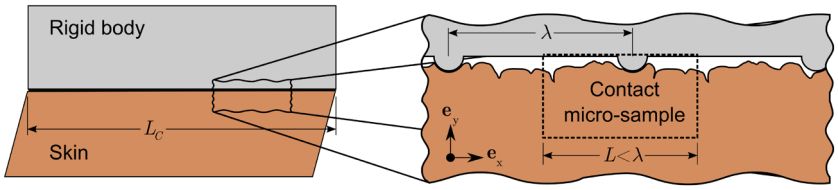

Figure 1. Schematic illustration of the rationale behind the contact homogenisation procedure used in this study. It consists of defining a representative section of the skin microstructure (length L) together with a rigid surface featuring rigid hemi-spherical rigid asperities separated by a distance $\lambda > L$. At the macroscopic scale (L_C), assembly of these periodic structures (individually referred as *contact micro-sample*) represent a macroscopic rigid body in contact with a macroscopic portion of skin.

$$\mu_g = \frac{F_T}{F_N} = \frac{\bar{f}_T \rho_a L_C}{\bar{f}_N \rho_a L_C} = \frac{\bar{f}_T}{\bar{f}_N}. \tag{4}$$

The pressure is obtained by dividing the normal component of the macroscopic traction vector by the total length of the contacting surface as:

$$P = \frac{F_N}{L_C} \tag{5}$$

which is equivalent to the pressure measured over the micro-sample:

$$P = \frac{\bar{f}_N}{\lambda}. \tag{6}$$

In order to get rid of the notion of wavelength λ (which can be chosen arbitrarily to some extent), we will use further in this paper the load $\bar{f}_N = P \cdot \lambda$ as an equivalent measure representing the pressure. For convenience, we will refer to this value as the equivalent pressure $P^* = P \cdot \lambda = \bar{f}_N$, measured in units of force or pressure length (i.e. [kPa·mm]).

2.2. Skin model

The finite element multi-layer skin model was based on anatomical geometry obtained from segmented histological sections of a dorsal skin sample of a 30-year-old Caucasian female as per our previous study [25]. This 1.982 mm-long skin section, referred as the region of interest (ROI), was embedded within a larger regular domain to avoid undesired boundary effects. This model captured the geometrical boundaries between the *stratum corneum*, viable epidermis and dermis, which was essential to calculate shear stress distribution across skin layers [3]. This came at the cost of a very fine mesh, thus requiring significant computing power. In the present study, because of the particular loading conditions and the scientific questions to be addressed, the distinction between the dermis and viable epidermis layers was unnecessary. The two layers were therefore merged together to form a single structure was meshed, together with the *stratum corneum* layer, within the pre/post-processing finite element environment of Abaqus/Standard 6.14 (Simulia, Dassault Systèmes, Providence, RI, USA). Care was applied to ensure sufficient mesh resolution for the *stratum corneum* (see figure 2) whilst reducing the number of elements in the viable epidermis-dermis composite structure. This resulted in a finite element model featuring only a third of the elements used in the former model [25] and therefore significantly reduced the computational cost per analysis.

The finite element mesh was exported to Mathematica® (Wolfram Research, Inc., Champaign, IL, USA) where finite deformation finite element simulations of skin contact interactions were conducted using the AceGen/AceFEM Mathematica® add-ons [33]. The contact element formulation was based on an Augmented Lagrangian technique [34, 35] for regularisation of unilateral contact constraints and the standard Newmark integration scheme for stabilising the solution procedure. The rigid indenter was assumed to be rigid while the skin layers were modelled as neo-Hookean materials, each featuring a ground state Young's modulus E and Poisson's ratio ν [36].

2.3. Simulation of sliding contact

As a preliminary step to each sliding simulation, the indenter was placed at a distance $s = 10^{-6}$ mm from the mean surface of the skin, and 0.2 mm on the left of the ROI, as shown in figure 3(a). Each finite element analysis consisted of three steps [32]. The indenter was subjected to:

1. A vertical translation D_y to induce a normal load and enforce contact between the skin surface and indenter (figure 3(b)). $D_y < 0$ indicates initial separation of the indenter from the skin surface and $D_y > 0$ initial indentation of the skin
2. A horizontal translation D_x^0 from the initial position to the left bound of the ROI in the deformed configuration, ensuring sliding conditions before entering this region (figure 3(c))
3. A horizontal translation D_x extended by 0.2 mm on the right of the ROI. The traction vector $\{f_N^i, f_T^i\}$ is measured at each discrete location along the sliding path within the ROI (figure 3(d)).

2.4. Design of computational experiment

The objectives of this large-scale series of parametric finite element analyses was to characterise the sensitivity of macroscopic skin friction to contact pressure, indenter size, microscopic friction and stiffness of the *stratum corneum*. The mechanical properties of the

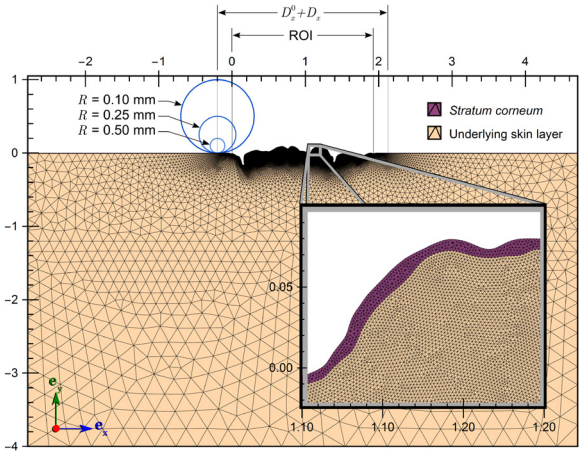

Figure 2. Finite element models of skin and indenters with model dimensions in mm. The three indenter sizes of radius $R = 0.1$, 0.25 and 0.5 mm are drawn to scale for reference. The anatomical geometry of the skin is contained at the top centre of the skin model, indicated by the region of interest (ROI). The distance $D_x^0 + D_x$ indicates the simulated total displacement of the indenter.

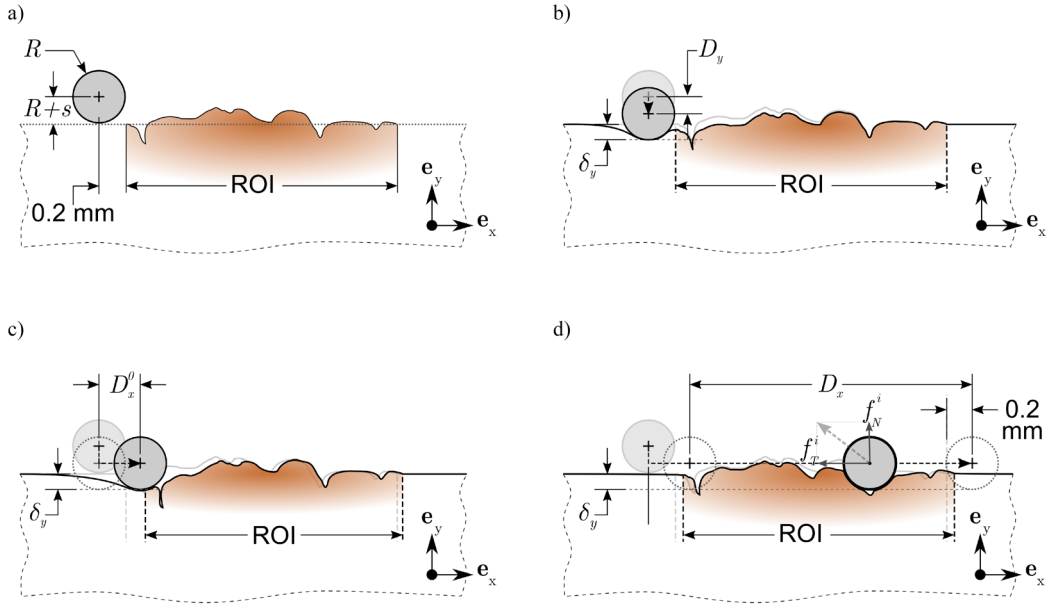

Figure 3. Simulation steps. (a) In the reference configuration, the indenter of radius R is placed at a distance s above the mean skin surface (dotted line) and 0.2 mm before the region of interest (ROI). (b) The indenter is vertically displaced by D_y, generating a skin displacement δ_y. (c) The indenter is horizontally displaced a distance D_x^0 until the edge of the ROI in the deformed configuration is reached. (d) The indenter ids horizontally displaced a distance D_x until it reaches a distance 0.2 mm outside the edge of the ROI in the reference configuration. The reference configuration is shown in light grey colour for steps (b)–(d).

skin substrate (i.e. composite assembly of dermis and viable epidermis) were fixed. The ground state Young's modulus and Poisson's ration were respectively $E_{\text{skin}} = 0.6$ MPa and $\nu = 0.3$ [4]. The variables considered, summarised in table 1, include:

- Young's modulus of the *stratum corneum* E_{SC} representing experimental values measured at 100% and 30% relative humidity levels [18]
- Indenter radius R to account for a range of indenter sizes commonly used in micro-indentation tests [37–39]
- Local coefficient of friction μ_1 representing a variety of contacting surfaces (such as nylon, plexiglass, steel, polyethylene, PVC, glass, among others) [2]
- Distance of the indenter surface from the undeformed mean surface of skin δ_y to account for a wide range of contact pressures P, represented by the equivalent pressure P^*.

A full factorial design of experiments was established leading to 312 finite element models and analyses.

2.5. Post-processing

The results of each finite element contact simulation were analysed to evaluate how the relation between the global coefficient of friction and pressure, referred from

Table 1. List of variables considered for the design of computational experiment: Young's modulus of the *stratum corneum* E_{SC}, asperity radius R, local coefficient of friction μ_l and distance between the mean surface of the skin and the nearest point of the asperity δ_y, where a negative sign indicates initial separation from the mean surface, and a positive one, initial indentation. A full-factorial design of experiment leads to 312 design variable combinations.

Variable	Values considered	Units
E_{SC}	0.6, 370	[MPa]
R	0.1, 0.25, 0.5	[mm]
μ_l	0.0, 0.1, 0.2, 0.3	[–]
δ_y	−0.07, −0.045, −0.023, 0, 0.01, 0.025, 0.05, 0.075, 0.1, 0.125, 0.15, 0.175, 0.2	[mm]

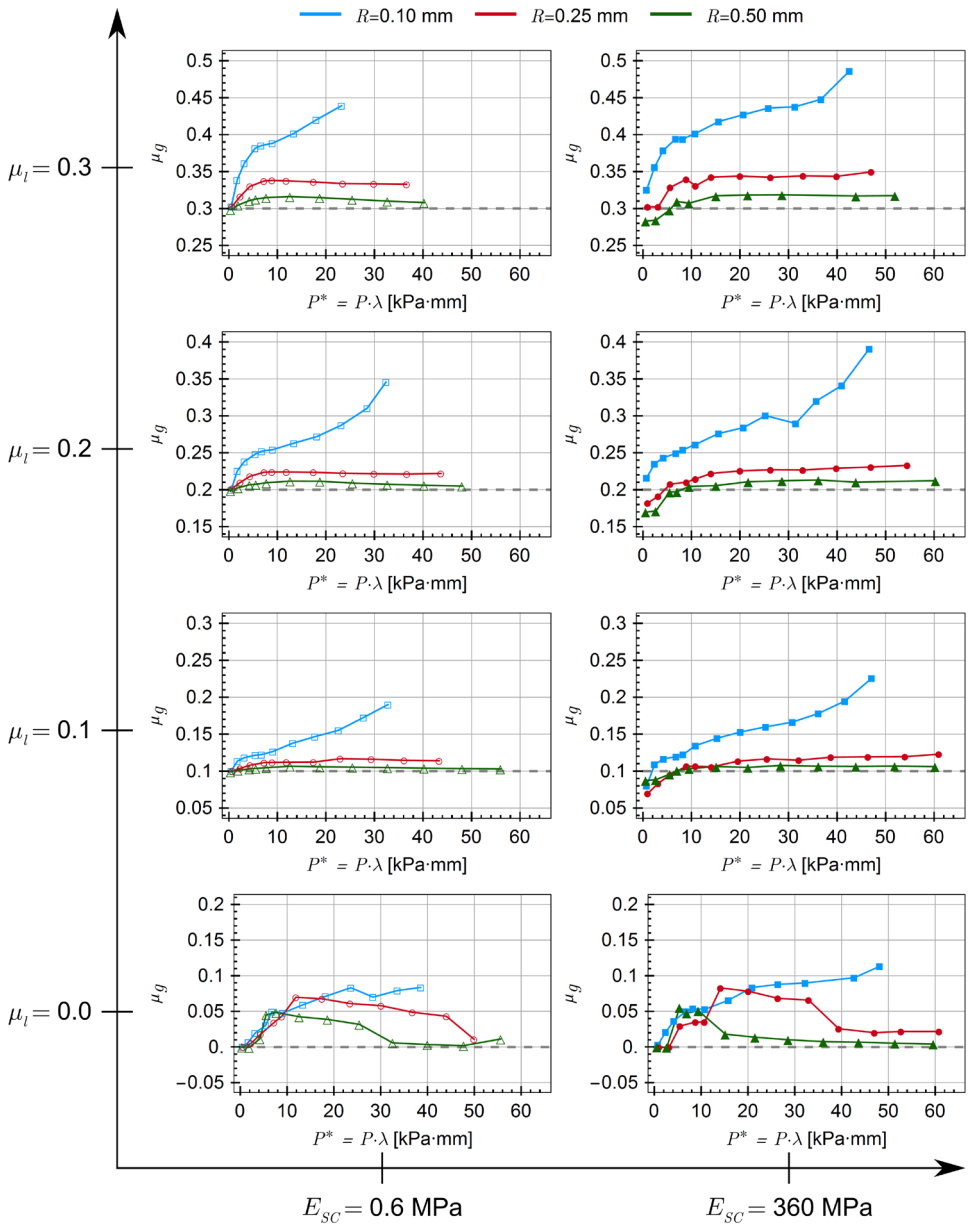

Figure 4. Variation of the global coefficient of friction μ_g as a function of equivalent pressure [kPa·mm] for the skin models featuring a *stratum corneum*'s Young's modulus of E_{SC} = 0.6 MPa (left) and those associated with E_{SC} = 370 MPa (right) as well as for local coefficients of friction from μ_l = 0.0 to μ_l = 0.3 (bottom to top).

now on as the friction-pressure relation, is affected by the skin microstructure (topography and changes in E_{SC}) and by each of the contact parameters considered (indenter size R and local coefficient of friction μ_l).

3. Results

Out of the 312 finite element analyses run as part of the full-factorial design of experiments (see

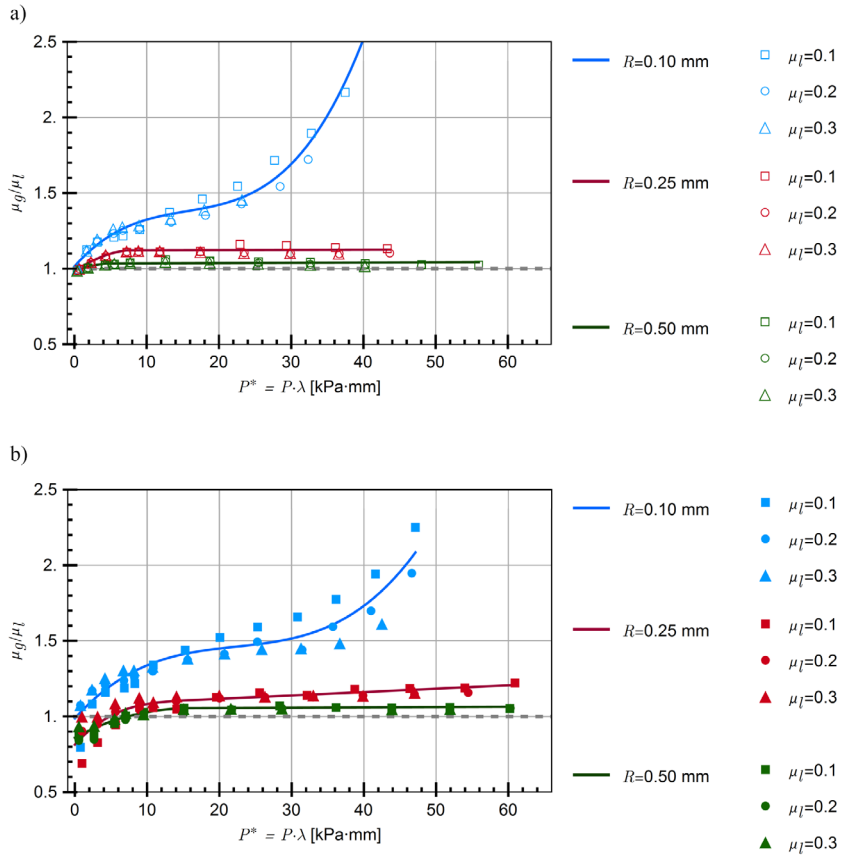

Figure 5. Normalised variation of the global coefficient of friction μ_g as a function of equivalent pressure [kPa·mm] for all of the analyses with (a) E_{SC} = 0.6 MPa and (b) E_{SC} =370 MPa, highlighting qualitative trend (solid lines) for each asperity size R and for each local coefficient of friction μ_l.

section 2.4), 287 completed successfully. Premature failure of some analyses were caused by numerical convergence problems, due to the highly non-linear nature of the contact problem combined with extreme relative softness of the skin layers. Besides dynamic regularisation, various strategies for adaptive load incrementation were used to improve the solving procedure. Failure to complete some analyses means that data points for the highest pressures considered are missing. Nevertheless, all the partially completed analyses provided sufficient information to extract trends relating macrosocopic friction to contact pressure and indenter size (figures 4 and 5). The results of the sliding contact simulations are presented in figure 4 as individual plots corresponding to every value of *stratum corneum*'s Young's modulus (left column: E_{SC} = 0.6 MPa; right column: E_{SC} = 370 MPa) and every value of local friction coefficient μ_l. Figure 5 is an alternative representation of the content of figure 4 in a normalised and more compact form (excluding the cases for $\mu_l = 0$). Table 2 summarises these results whilst also providing additional information.

3.1. Contribution of the skin microstructure to the macroscopic coefficient of friction

The results of the simulations featuring no local friction ($\mu_l = 0$) are presented in figure 4 (bottom plots). Strikingly, for both left and right plots, it can be observed that macroscopic friction is non null despite the absence of local friction. Macroscopic friction μ_g increases non-linearly with pressure up to a critical pressure value P_C which is indenter size- and pressure-dependent. Beyond this critical pressure, for the two largest indenter sizes (R =0.25 mm and R = 0.5 mm), μ_g drops down to a second critical pressure, henceforth referred as *plateau pressure* P_P, which marks the beginning of a plateau phase where μ_g becomes mostly constant, therefore insensitive to increasing pressure. For the smallest indenter (R = 0.1 mm), after reaching P_C, μ_g continues to increase with pressure, albeit at a smaller rate. Results clearly show that macroscopic friction tend to increase as indenter radius decreases but, for the largest indenters, after a critical pressure value is reached, friction becomes less sensitive to pressure. There is an intrinsic coupling between friction forces and finite deformations of skin asperities that will be discussed in section 4, even when there is no local friction. This effectively demonstrates that skin microstructure contributes to friction via mechanisms purely induced by deformation as it has been previously shown in similar computational studies [3,4]. The effect of *stratum corneum* Young's modulus on macroscopic friction is evidenced by comparing the frictionless plots ($\mu_l = 0$) in figure 4 for E_{SC} = 0.6 MPa (left) and

Table 2. Summary of numerical results for each case with a given local coefficient of friction (μ_l), Young's modulus of the *stratum corneum* (E_{SC}) and asperity radius (R), showing the maximum and minimum global coefficient of friction (μ_g^{max} and μ_g^{min}, respectively) and the pressure P at which they were recorded, the plateau pressure P_P and the average global coefficient of friction after P_P. (NA: not applicable).

Case								
μ_l	E_{SC} [MPa]	R [mm]	μ_g^{min}	P at μ_g^{min} [kPa·mm]	μ_g^{max}	P at μ_g^{max} [kPa·mm]	P_P [kPa·mm]	Plateau μ_g
0.0	0.6	0.10	$1.8 \cdot 10^{-4}$	0.483	0.084	38.538	NA	NA
0.0	0.6	0.25	$2.6 \cdot 10^{-5}$	0.652	0.070	11.884	NA	NA
0.0	0.6	0.50	$-3.7 \cdot 10^{-4}$	1.908	0.048	7.685	44.02	0.043
0.0	370	0.10	$3.1 \cdot 10^{-3}$	0.770	0.113	48.132	NA	NA
0.0	370	0.25	$-4.7 \cdot 10^{-4}$	0.992	0.083	14.166	47.03	0.021
0.0	370	0.50	$-3.1 \cdot 10^{-4}$	2.658	0.055	5.398	15.17	0.009
0.1	0.6	0.10	0.100	0.483	0.278	41.662	NA	NA
0.1	0.6	0.25	0.100	0.652	0.117	22.942	7.27	0.114
0.1	0.6	0.50	0.099	0.367	0.107	12.643	0.37	0.104
0.1	370	0.10	0.080	0.770	0.226	47.144	NA	NA
0.1	370	0.25	0.070	0.994	0.123	60.951	14.12	0.116
0.1	370	0.50	0.087	0.575	0.108	28.373	7.05	0.105
0.2	0.6	0.10	0.200	0.482	0.346	32.374	NA	NA
0.2	0.6	0.25	0.202	0.652	0.224	8.902	7.25	0.223
0.2	0.6	0.50	0.199	0.368	0.212	12.633	4.25	0.208
0.2	370	0.10	0.216	0.769	0.391	46.656	NA	NA
0.2	370	0.25	0.182	0.994	0.233	54.465	14.05	0.228
0.2	370	0.50	0.170	0.576	0.213	36.156	9.52	0.210
0.3	0.6	0.10	0.303	0.479	0.439	23.210	NA	NA
0.3	0.6	0.25	0.303	0.651	0.338	8.875	7.23	0.336
0.3	0.6	0.50	0.298	0.368	0.316	12.608	4.24	0.313
0.3	370	0.10	0.325	0.769	0.486	42.531	NA	NA
0.3	370	0.25	0.302	3.150	0.350	47.064	14.08	0.344
0.3	370	0.50	0.283	0.578	0.319	28.678	15.06	0.318

$E_{SC} = 370$ MPa (right). First, for the same level of vertical displacement δ_y, and as expected, pressure is higher for the stiffer outer layer. Second, the global coefficient of friction tends to increase with the Young's modulus of the *stratum corneum*. Third, the simulations with the stiffer *stratum corneum* exhibited lower values of the critical and plateau pressures than those for the softer *stratum corneum*. It is pertinent to point out that, in these conditions, the increased elastic modulus of the *stratum corneum* creates the hard-soft layered structure of the skin, for which the skin's equivalent (i.e. composite) Young's modulus is higher than 0.6 MPa.

3.2. Friction-pressure relation for non-frictionless surfaces

The results of the simulations featuring contact surfaces endowed with local friction ($\mu_l > 0$) are also presented in figure 4. For both values of the *stratum corneum*'s Young's modulus, the numerical analyses show consistent trends for the three values of local friction (0.1, 0.2 and 0.3). The global coefficient of friction increases nonlinearly at low pressures up to a critical pressure P_C. In contrast to the simulations with local frictionless contact, these simulations did not show a steep decrease in friction at $P > P_C$, but they rather reach a plateau stage at this point (i.e. $P_C = P_P$), beyond which macroscopic friction becomes mostly constant. For the smallest indenter size ($R = 0.1$ mm), the response of global friction as a function of pressure is markedly non-linear with a steep increase in the low-pressure regime, followed by another non-linear phase but with a much-reduced rate of increase. Again, this is to analyse in relation to finite deformations of skin asperities and underlying bulk material, where geometrical constraints oppose motion of the sliding indenter. The macroscopic friction for the smallest indenter size ($R = 0.1$ mm) is also significantly higher than for the two other indenter sizes and for every local friction coefficient considered. Interactions of the indenter with the skin microstructure modulate the effects of local friction and magnify macroscopic friction. For the two largest indenter sizes considered, once the plateau phase has been reached, the macroscopic friction coefficient is very close to the assigned microscopic friction coefficient. By comparing the left ($E_{SC} = 0.6$ MPa) and right ($E_{SC} = 370$ MPa) plots for $\mu_l > 0$ in figure 4, the role of the *stratum corneum* Young's modulus in modulating macroscopic friction is apparent. As in the cases with no local friction, macroscopic friction increases with stiffening of the *stratum corneum*.

One can observe that, in figure 4 (right) for $\mu_l = 0.1$, all the curves start at a global coefficient of friction $\mu_g < \mu_l$, but as the local coefficient of friction gets higher, this effect is only observed for the case with larger indenter sizes ($R = 0.25$ mm and $R = 0.5$ mm). As pressure increases, macroscopic friction overtakes microscopic friction ($\mu_g > \mu_l$). Similar counter-intuitive effects have also been observed in other studies [4, 32].

3.3. Normalised coefficient of friction-pressure curves

For the contact analyses featuring a non-zero local coefficient of friction, the calculated global coefficient of friction was normalised by its corresponding local coefficient of friction, as in Stupkiewicz *et al* [32], in order to get a more insightful understanding of qualitative trends. The normalised macroscopic friction μ_g^* is calculated as:

$$\mu_g^* = \mu_g/\mu_l \tag{7}$$

These normalised results are illustrated in figures 5(a) and (b), respectively for the simulations with $E_{SC} = 0.6$ MPa and $E_{SC} = 360$ MPa. Although Stupkiewicz *et al* [32] related the applied pressure to the reduced Young's modulus of the soft material ($E^* = E/(1-\nu^2)$), this approach cannot be straightforwardly applied for the skin with the stiffer *stratum corneum*, as effective elastic properties of the skin would depend on the thickness of this outer layer and depth of indentation [40, 41].

Using the best-fit trends indicated by the solid lines in figure 5, one can see that μ_g^* features insignificant variations in the plateau stage captured for the medium and large indenter sizes ($R = 0.25$ mm and $R = 0.5$ mm) whilst clearly exhibiting a non-linear response over the whole pressure range for the smallest one. However, in the low-pressure regime (more clearly observed for the simulations with $R = 0.10$ mm) there is some dispersion for μ_g^* depending on the local coefficient of friction μ_l. For the stiffest *stratum corneum* case (figure 5(b)), at the origin of the plots ($P \to 0$ kPa·mm), the normalised coefficient of friction is lower than unity indicating that, despite the existence of local friction forces, they are not amplified and propagated to the macroscopic scale, but are rather down-modulated.

4. Discussion

In this study, we performed a systematic multi-parametric computational analysis to investigate the sensitivity of the macroscopic coefficient of friction of human skin to a wide range of loading and contact conditions as well as for two extreme cases of stiffness for the *stratum corneum* layer. Intrinsic parameters of the system that were varied included the Young's modulus for the *stratum corneum* E_{SC}, the local coefficient of friction μ_l between the skin surface and that of the indenter, as well as the rigid indenter size R. Using a finite element computational approach including contact homogenisation [4], we simulated sliding contact of a rigid indenter over a 2D anatomically-based skin model obtained from a histological sample of human skin [25]. The extrinsic parameter to the system was the indentation depth δ_y from the skin's surface, taken as a surrogate measure of contact pressure. Up to thirteen values of δ_y were considered for each combination of E_{SC}, μ_l and R. This resulted in a full-factorial design of experiment featuring 312 individual finite element analyses. For the 13 analyses of each given combination of E_{SC}, μ_l and R, a macroscopic friction-pressure curve was extracted (figures 4 and 5).

As expected, results of the analyses were consistent with those obtained in our previous computational studies [3, 4]. Finite deformations of asperities of the skin and, more generally, that of its surface and internal microstructure can generate significant resistance forces in response to the sliding motion of a rigid indenter of sub-millimetric size. Skin asperities act as geometrical constraints that oppose indenter motion but, because they can undergo significant finite deformations, the net macroscopic force applied to the indenter is heavily modulated as each asperity rebalance local reaction forces during its deformation. Skin deformations are not restricted to asperities but also propagate from the *stratum corneum* surface to the deeper layer. This mechanical response is intrinsically linked to the mechanical properties of each skin layer and this was clearly demonstrated by considering two extreme values of Young's modulus for the *stratum corneum*. Macroscopic friction was found to increase with the material stiffness of the *stratum corneum* layer.

Three key observations could be made from the results:

- For the smallest indenter size considered, which was comparable to the characteristic size of the skin roughness, the global coefficients of friction were higher and the plateau stage, where friction becomes mostly constant, was not observed at the analysed pressure levels. This means that for the smallest asperities of a contacting surface the global friction is not only higher, but also remains sensitive to pressure for a wider range of pressures than for the case of larger asperities.
- For a stiffer *stratum corneum*, the global friction response can be reduced at lower pressures by favouring long-range macroscopic structural deformations (e.g. bending of the whole *stratum corneum* layer) over localised deformations (e.g. those of microscopic asperities). However, this behaviour can be counteracted and neutralised by the effects of indenter size to that of skin surface asperities. This illustrates ad reveals the complex physical interplay of some of the multiple factors governing and modulating skin friction. These

mechanisms operate, first at a local scale, and then at a macrosocopic scale.
- As the local friction coefficient increases, the difference between the local and global coefficients of friction increase non-linearly. This means that the local coefficient of friction, in combination with the softness and, therefore, propensity to deform, of the skin asperities is an important modulator of the macroscopic friction response.

Historically, it has often been assumed that skin surface roughness does not significantly contribute to its friction behaviour [2] because the soft skin surface is believed to *adapt* to any stiffer (by several orders of magnitude) contacting surface. The logic underlying this hypothesis is that high surface conformity lead to a dominance of adhesive surface forces over reaction forces, induced by resistance and deformations of skin asperities. Although the current and previous studies of our group [3, 4] did not *explicitly* include adhesive forces, they have shown that purely elastic deformations of skin asperities endowed with local friction properties can create significant resistance to a rigid indenter sliding motion and, by so doing, induce friction forces. This is accomplished by the action of the indenter (that could also be viewed as a single rigid asperity) that creates local skin deformations by entrainment of the skin surface and modulates the local stiffness of the skin microstructure. In turn, this induces particular kinematics constraints that resists indenter motion and produce friction forces. Although several researchers [2, 42] also recognise the fundamental aspects of these deformation-induced mechanisms they rather consider them in terms of the asperities of the external surface s rather than those of the skin.

At this stage, it is relevant to reiterate that we did not model adhesion *explicitly*, however, it was *implicitly* accounted for as a smeared physical contribution included in the local coefficient of friction. The local (i.e. microscopic) coefficient of friction could be viewed as the homogenised version of a friction descriptor encompassing deformation-induced and adhesive forces arising from a smaller length scale (i.e. nanoscopic).

Other researchers [6, 43, 44] conducted physical experiments to measure skin friction *in vivo* and concluded that the coefficient of friction between the skin and a wide range of surfaces is determined by the geometrical characteristics of the contacting surface rather than those of the skin. Our current and previous results [3, 4] showed that the skin microstructure does contribute to its friction behaviour against a rigid slider. Here, it was shown how the level of pressure modulates these effects, and also, how it induces a cross-talk with the relative size of the indenter compared to those of skin asperities, and also with the stiffness of the *stratum corneum* layer. It is therefore essential to emphasise that the frictional properties of skin against external surfaces cannot be reported as absolute quantities. They are dependent upon many intrinsic physical factors including material and microstructural properties, as well as external factors such as loading and environmental conditions.

In reality, macroscopic friction arises as the result of complex, multiscale, multiphysics, dissipative as well as conservative phenomena that, by definition, encompass a large number of physical parameters [10, 17]. Here, our computational study focused on a restricted subset of these parameters, but this seemingly limiting assumption is also a strength. By placing the focus of our computational experiment on the micromechanics of skin deformations in response to the sliding motion of a rigid indenter, we were able to isolate the effects of geometry, material properties, pressure and microscopic surface properties (i.e. local friction).

The ability to conduct systematic parametric studies is one of the major attractive and defining aspects of computational modelling, particularly if considering large-scale experiments that would be impossible, too lengthy or too costly to reproduce in a physical experimental setting. For example, van Kuilenburg *et al* [44] designed surfaces with specific geometrical characteristics (e.g. asperity radius and distance between asperities) and used them to conduct skin finger pad friction experiments at various levels of contact force. The challenges of conducting high-throughput physical experiments of this nature are obvious and, in that particular study, meant that only a limited number of data points describing macroscopic friction were available. This was insufficient to establish conclusive trends for macroscopic friction in terms of surface asperities' characteristics an applied load.

Another significant shortcoming of physical experiments is embodied by the difficulty in ensuring reproducibility of results because of system and experiment variability coupled to the high sensitivity of skin to environmental conditions. A computational approach can fill those gaps and also increase the number of computational experiments according to the requirements of the study and availability of computational resources.

In this study, we established a design of experiments consisting of 312 numerical simulations, of which 287 accounted for the whole range of contact pressures considered at the outset. Finite element contact analyses of soft matter are notoriously technically challenging [45, 46]. This is due to potentially significant finite deformations associated to high stiffness ratios which lead to highly non-linear structural behaviour under the form of instabilities (e.g. snap-back and snap-through).

Inherent to any mathematical or computational model, are the necessary simplifications which restrict its domain of validity in terms of the physical processes captured (e.g. dissipative inelastic effects) and/or the particular conditions simulated (e.g. loading

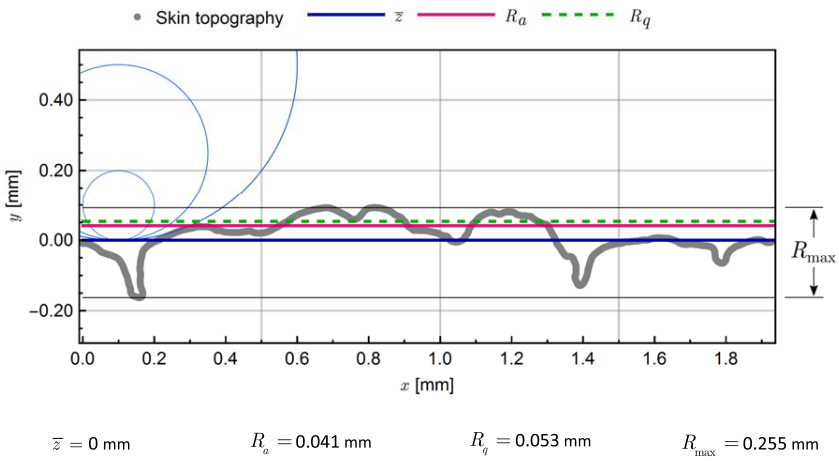

Figure 6. Surface characteristics of the skin sample used in this study: mean surface $\bar{z}$, surface roughness R_a, RMS roughness R_q and maximum peak-to-valley height R_{max}. $\bar{z} = 0$ mm, $R_a = 0.041$ mm, $R_q = 0.053$ mm, $R_{max} = 0.255$ mm.

conditions). In the current model, we did not consider the 3D geometry of the skin surface nor its internal microstructure (e.g. distinct viable epidermis and dermis layers). Therefore this precluded the complex 3D structural deformation effects [1, 47] that would naturally arise, particularly if anisotropic material properties and structural heterogeneities were accounted for. Their effects on deformation-induced friction would be expected as well as the introduction of anisotropic frictional forces [32]. We also restricted our constitutive framework to non-linear isotropic elasticity. The viscoelastic and other dissipative (e.g. plasticity and poroelasticity) properties of the skin are known to play a fundamental role in its rheology and tribology [2]. At this stage, in order to study structural mechanisms associated with deformation-induced friction, introduction of these material properties was unnecessary and would have rendered interpretation of our large-scale computational experimental less straightforward. Future studies should definitely consider viscoelastic properties, particularly in combination with finite deformations and a wide range of sliding velocities [5].

Most of the skin tribology community and associated literature have consistently assumed that skin friction can be decomposed into an adhesion component which encompasses surface physical forces [17, 48, 49] and an hysteretic component which represents dissipative effects [14, 22]. It appears relevant to highlight that, despite the definite contribution of dissipative phenomena to friction forces, purely conservative behaviour such as elasticity can also contribute to friction forces by modulating the shape of surfaces and volumes.

The take-home message of our study is that skin friction is a complex phenomenon that requires a full 3D geometrical and material approach if one aims to establish a *mechanistic* understanding of it. Because skin friction [48] is intrinsically linked to surface and bulk deformations of its heterogeneous microstructure, only a full 3D finite deformation setting can capture these effects, even if down the line this lead to simplified scalar descriptors of friction (e.g. macroscopic coefficients of friction). This is true whether one considers deformation-induced, hysteretic and/or adhesion components of friction. Mechanical deformations (i.e. geometrical effects) are essential in what is a multiphysical problem. Although analytical and semi-analytical models of rubber [9, 11, 50] and skin [12, 51] friction have been pivotal in advancing our understanding of contact mechanics of soft matter, they present *a priori* limitations because of their failure to account for other than linear elastic materials, and geometrical effects which are critically important as evidenced in the present and previous computational studies on skin [3, 4, 25] or other comparable general approaches based on multiscale finite element techniques [13, 14, 45, 46, 52].

Results of the computational analyses have shown that the size of the rigid indenter matters in controlling the macroscopic frictional response. Here, it is of course a matter of *relative* size of indenter compared to those of skin asperities. As the size of the indenter increases, mechanical interactions (e.g. kinematic constraints/interlocking) between indenter and skin asperities transition from local to global (i.e. macroscopic). Mechanical loads are distributed over many more asperities so that the whole skin surface deforms. Our skin sample has a surface roughness $R_a = 0.041$ mm and a root mean squared roughness of $R_q = 0.053$ mm (see figure 6). In comparison to its maximum surface height $R_{max} = 0.255$ mm, the ratio between the smaller asperity ($R = 0.10$ mm) and R_{max} is approximately 0.4, while for other asperities this ratio is larger than one. Higher resistance is expected when $R \simeq R_a$ due to interlocking of the indenter (i.e. asperity) with the skin topographic features. In our results, for the minimal contact stiffness (arising from the lowest value of E_{SC}, $E_{SC} = 0.6$ MPa) lower friction values were obtained compared to the case where $E_{SC} = 370$ MPa. Therefore, it is expected that for a given contacting surface, skins with deeper fur-

rows but softer bulk response (lower contact stiffness) would exhibit a similar friction response. This was experimentally observed by Gerhardt *et al* [53].

The friction-pressure trend identified in our results indicates that the skin frictional response is very sensitive to variations in pressure. For the case $R \simeq R_a$ it can be observed in the whole analysed spectrum of pressures. For the case $R \gg R_a$ the effects are clear in the low-pressure regime only and the pressure dependency fades away as pressure further increases. This corroborates experimental observations by Wolfram [7].

At low pressure, interlocking is the principal mechanism of resistance to indenter motion. At higher pressure, the asperities of the skin surface reach a critical level of deformation and strain whereby deformations propagate deeper into the skin tissue, so the motion resistance generated by this deformation is mostly no longer sensitive to pressure. Of course, these mechanisms are not so sharply defined and the interplay is complex but this simplified explanation captures the essence of what physically happens. This trend was documented by Adams *et al* [22], for their experimental friction measurements of polypropylene and glass on skin in dry conditions. From their experimental study, Egawa *et al* [54] concluded that moisture of the skin has a dominant effect on skin friction over that of skin's topographic features. Like in the present study, these authors also observed a plateau stage in the description of measured friction as a function of applied pressure loads.

The low-pressure regime of the trend was also reported from the computational study on anisotropic contact of rubber-like materials of Stupkiewicz *et al* [32]. They showed that, depending on the rubber surface characteristics, the low-pressure regime in the friction-pressure relation can vary from a sigmoidal-type increase of to a complex S-shaped curve. These observations corroborate the characteristics of the friction-pressure curves seen our non-frictionless simulations with the softer and stiffer *stratum corneum*, respectively. Moreover, the typical peak contact pressures measured for people sitting on (6.4–26 kPa) [55] and laying on (approximately 7.7 kPa) [56] a soft surface, patients with spinal cord injuries siting on a cushioned wheelchair (20–30 kPa) [55], and normal subjects sitting on a rigid surface (approximately 40 kPa). This is comparable to the pressures simulated in our computational experiment (up to 61 kPa for a hypothetical $\lambda = 1$ mm).

As alluded to multiple times in this paper, skin friction arises from the multiscale interplay of many types of physical processes ranging from intermolecular forces to macroscopic structural deformations. The respective contribution of each of these physical mechanisms to macroscopic friction is dynamic and depends on both intrinsic (e.g. material and structural properties) and extrinsic parameters (e.g. applied pressure, relative humidity). In a skin health/comfort context, this has very important implications as excessive friction forces can be detrimental to the structural integrity of skin and, ultimately, to health [57, 58]. For a given surface in contact with the skin, the tribological response will vary depending on the intra- and inter-individual skin characteristics [3, 4] besides external factors such as temperature or relative humidity [30]. The fact that certain categories of people (e.g. aged population, bed-ridden patients) are more prone to develop friction-associated skin injuries is a clear testimony of that [59].

5. Conclusion

In this study, we performed a large-scale multi-parametric computational analysis to systematically investigate the sensitivity of the macroscopic coefficient of friction of human skin to a wide range of loading and contact conditions as well as for two extreme cases of stiffness for the *stratum corneum* layer. The generic finite element model used was based on an anatomically-based 2D histological section of human skin, thus capturing the complex skin microstructure and surface topography which was shown to be pivotal in modulating deformation-induced macroscopic skin friction. For the analyses considering an indenter radius similar to the characteristic length of the skin roughness, the macroscopic friction is very sensitive to pressure. For larger indenter radii that dependency is evident at low pressures, whilst it mostly disappears as pressure increases beyond a critical value. The contact homogenisation procedure confirmed the potentially major role of finite deformations of skin asperities on the resulting macroscopic friction. This effect was shown to be modulated by the level of contact pressure and the relative size of skin surface asperities compared to those of a rigid indenter, or, by taking a broader view, to asperities of the contacting surfaces. As per our previous studies [3, 4] and those found in the literature relevant to computational soft matter physics [13, 14, 45, 46, 52], this study highlighted the importance of accounting for detailed surface geometries and deformations in order to gain a *mechanistic* insight into the complexity of friction.

Future extensions of the model will include 3D geometries and multiple rigid and deformable asperities. The use of a larger population of skin micro-samples will also be essential to capture intra-individual and inter-individual variability, particularly in relations to age-dependent material and structural properties [60, 61]. Prior to that, the inclusion of finite strain viscoelasticity would also be a logical addition to our contact homogenisation framework. The study presented in this paper is a logical progression toward the development of physics-based simulation tools to investigate fundamental aspects of skin friction and also to assist design engineers in tuning and optimising products intended to interact with the skin. Our computational modelling platform offers attractive

features which are beyond the reach of current analytical mathematical models of skin friction, namely, the ability to accommodate arbitrary kinematics (i.e. finite deformations), non-linear constitutive properties and the complex geometry of the skin microstructural constituents.

Acknowledgements

Maria-Fabiola Leyva-Mendivil was supported by a CONACyT fellowship (Grant 077913) and an EPSRC Institutional Sponsorship Award (University of Southampton). The financial support of these organisations is gratefully acknowledged. The authors would like to acknowledge the numerous fruitful discussions on skin friction with Dr David-John O'Callaghan of Procter and Gamble. The authors would also like to thank the editors for the invitation to contribute to this special issue.

Data access statement

All data supporting this study are openly available from the University of Southampton repository at https://doi.org/10.5258/SOTON/D0285.

ORCID iDs

Maria F Leyva-Mendivil https://orcid.org/0000-0002-9964-7730

References

[1] Limbert G 2017 Mathematical and computational modelling of skin biophysics-a review *Proc. R. Soc.* A **473** 1–39
[2] Derler S and Gerhardt L C 2012 Tribology of skin: review and analysis of experimental results for the friction coefficient of human skin *Tribol. Lett.* **45** 1–27
[3] Leyva-Mendivil M F, Lengiewicz J, Page A, Bressloff N W and Limbert G 2017 Implications of multi-asperity contact for shear stress distribution in the viable epidermis—an image-based finite element study *Biotribology* **11** 110–23
[4] Leyva-Mendivil M F, Lengiewicz J, Page A, Bressloff N W and Limbert G 2017 Skin microstructure is a key contributor to its friction behaviour *Tribol. Lett.* **65** 12
[5] Van der Heide E, Zeng X and Masen M A 2013 Skin tribology: science friction? *Friction* **1** 130–42
[6] Veijgen N K, Masen M A and van der Heide E 2013 Variables influencing the frictional behaviour of *in vivo* human skin *J. Mech. Behav. Biomed. Mater.* **28** 448–61
[7] Wolfram L J 1983 Friction of skin *J. Soc. Cosmet. Chem.* **34** 465–76
[8] Morey P 2007 Skin tears: a literature review *Primary Intention* **15** 122–9
[9] Persson B N J 1998 On the theory of rubber friction *Surf. Sci.* **401** 445–54
[10] Persson B N J 2000 *Sliding Friction* (Berlin: Springer) (https://doi.org/10.1007/978-3-662-04283-0)
[11] Persson B N J 2001 Theory of rubber friction and contact mechanics *J. Chem. Phys.* **115** 3840–61
[12] Persson B N J, Kovalev A and Gorb S N 2013 Contact mechanics and friction on dry and wet human skin *Tribol. Lett.* **50** 17–30
[13] Wagner P, Wriggers P, Klapproth C, Prange C and Wies B 2015 Multiscale FEM approach for hysteresis friction of rubber on rough surfaces *Comput. Methods Appl. Mech. Eng.* **296** 150–68
[14] Wagner P, Wriggers P, Veltmaat L, Clasen H, Prange C and Wies B 2017 Numerical multiscale modelling and experimental validation of low speed rubber friction on rough road surfaces including hysteretic and adhesive effects *Tribol. Int.* **111** 243–53
[15] Greenwood J A and Tabor D 1958 The friction of hard sliders on lubricated rubber: the importance of deformation losses *Proc. Phys. Soci.* **71** 989–1001
[16] Greenwood J A, Minshall H and Tabor D 1961 Hysteresis losses in rolling and sliding friction *Proc. R. Soc.* A **259** 480–507
[17] Israelachvili J N 1991 *Intermolecular and Surface Forces* 2nd edn (Amsterdam: Elsevier)
[18] Wu K S, van Osdol W W and Dauskardt R H 2006 Mechanical properties of human stratum corneum: effects of temperature, hydration, and chemical treatment *Biomaterials* **27** 785–95
[19] Levi K, Weber R J, Do J Q and Dauskardt R H 2010 Drying stress and damage processes in human stratum corneum *Int. J. Cosmetic Sci.* **32** 276–93
[20] Li X, Johnson R, Weinstein B, Wilder E, Smith E and Kasting G B 2015 Dynamics of water transport and swelling in human stratum corneum *Chem. Eng. Sci.* **138** 164–72
[21] Liu X, Cleary J and German G K 2016 The global mechanical properties and multi-scale failure mechanics of heterogeneous human stratum corneum *Acta Biomater.* **43** 78–87
[22] Adams M J, Briscoe B J and Johnson S A 2007 Friction and lubrication of human skin *Tribol. Lett.* **26** 239–53
[23] Flynn C and McCormack B A O 2008 Finite element modelling of forearm skin wrinkling *Skin Res. Technol.* **14** 261–9
[24] Flynn C O and McCormack B A O 2009 A three-layer model of skin and its application in simulating wrinkling *Comput. Methods Biomech. Biomed. Eng.* **12** 125–34
[25] Leyva-Mendivil M F, Page A, Bressloff N W and Limbert G 2015 A mechanistic insight into the mechanical role of the stratum corneum during stretching and compression of the skin *J. Mech. Behav. Biomed. Mater.* **49** 197–219
[26] Levi K, Kwan A, Rhines A S, Gorcea M, Moore D J and Dauskardt R H 2010 Emollient molecule effects on the drying stresses in human stratum corneum *Br. J. Dermatol.* **163** 695–703
[27] Wu K S H 2006 Mechanical behavior of human stratum corneum: relationship to tissue structure and condition *PhD Thesis* Stanford University (http://adsabs.harvard.edu/abs/2006PhDT.....73W)
[28] Veijgen N K, Masen M A and van der Heide E 2013 Relating friction on the human skin to the hydration and temperature of the skin *Tribol. Lett.* **49** 251–62
[29] Gerhardt L C, Strässle V, Lenz A, Spencer N D and Derler S 2008 Influence of epidermal hydration on the friction of human skin against textiles *J. R. Soc. Interface* **5** 1317–28
[30] Gefen A 2011 How do microclimate factors affect the risk for superficial pressure ulcers: a mathematical modeling study *J. Tissue Viability* **20** 81–8
[31] Yusuf S *et al* 2015 Microclimate and development of pressure ulcers and superficial skin changes *Int. Wound J.* **12** 40–6
[32] Stupkiewicz S, Lewandowski M J and Lengiewicz J 2014 Micromechanical analysis of friction anisotropy in rough elastic contacts *Int. J. Solids Struct.* **51** 3931–43
[33] Korelc J 2002 Multi-language and multi-environment generation of nonlinear finite element codes *Eng. Comput.* **18** 312–27
[34] Lengiewicz J, Korelc J and Stupkiewicz S 2011 Automation of finite element formulations for large deformation contact problems *Int. J. Numer. Methods Eng.* **85** 1252–79
[35] Newmark N M 1959 A method of computation for structural dynamics *J. Eng. Mech. Div.* **85** 67–94
[36] Holzapfel G A 2004 *Nonlinear Solid Mechanics: a Continuum Approach for Engineering* (Chichester: Wiley)
[37] Clancy N T, Nilsson G E, Anderson C D and Leahy M J 2010 A new device for assessing changes in skin viscoelasticity using indentation and optical measurement *Skin Res. Technol.* **16** 210–28
[38] Geerligs M, van Breemen L, Peters G, Ackermans P, Baaijens F and Oomens C 2011 *In vitro* indentation to

determine the mechanical properties of epidermis *J. Biomech.* **44** 1176–81
[39] Iivarinen J T, Korhonen R K, Julkunen P and Jurvelin J S 2011 Experimental and computational analysis of soft tissue stiffness in forearm using a manual indentation device *Med. Eng. Phys.* **33** 1245–53
[40] Bhushan B 2012 Nanotribological and nanomechanical properties of skin with and without cream treatment using atomic force microscopy and nanoindentation *J. Colloid Interface Sci.* **367** 1–33
[41] Yuan Y and Verma R 2006 Measuring microelastic properties of stratum corneum *Colloids Surf.* B **48** 6–12
[42] Tomlinson S E, Carré M J, Lewis R and Franklin S E 2011 Human finger contact with small, triangular ridged surfaces *Wear* **271** 2346–53
[43] Veijgen N K, van der Heide E and Masen M A 2013 A multivariable model for predicting the frictional behaviour and hydration of the human skin *Skin Res. Technol.* **19** 330–8
[44] van Kuilenburg J, Masen M A and van der Heide E 2013 The role of the skin microrelief in the contact behaviour of human skin: contact between the human finger and regular surface textures *Tribol. Int.* **65** 81–90
[45] Kiliç K I and Temizer I 2016 Tuning macroscopic sliding friction at soft contact interfaces: interaction of bulk and surface heterogeneities *Tribol. Int.* **104** 83–97
[46] Temizer I 2014 Computational homogenization of soft matter friction: isogeometric framework and elastic boundary layers *Int. J. Numer. Methods Eng.* **100** 953–81
[47] Limbert G and Kuhl E 2017 On skin microrelief and the emergence of expression micro-wrinkles *Soft Matter* accepted (http://doi.org/10.1039/C7SM01969F)
[48] Pailler-Mattéi C and Zahouani H 2004 Study of adhesion forces and mechanical properties of human skin *in vivo* *J. Adhes. Sci. Technol.* **18** 1739–58
[49] Pailler-Mattéi C and Zahouani H 2006 Analysis of adhesive behaviour of human skin *in vivo* by an indentation test *Tribol. Int.* **39** 12–21
[50] Persson B N J and Scaraggi M 2014 Theory of adhesion: role of surface roughness *J. Chem. Phys.* **141** 124701
[51] Kovalev A E, Dening K, Persson B N J and Gorb S N 2014 Surface topography and contact mechanics of dry and wet human skin *Beilstein J. Nanotechnol.* **5** 1341–8
[52] Temizer I 2016 Sliding friction across the scales: thermomechanical interactions and dissipation partitioning *J. Mech. Phys. Solids* **89** 126–48
[53] Gerhardt L C, Lenz A, Spencer N D, Münzer T and Derler S 2009 Skin-textile friction and skin elasticity in young and aged persons *Skin Res. Technol.* **15** 288–98
[54] Egawa M, Oguri M, Hirao T, Takahashi M and Miyakawa M 2002 The evaluation of skin friction using africtional feel analyzer *Skin Res. Technol.* **8** 41–51
[55] Gefen A 2007 Pressure-sensing devices for assessment of soft tissue loading under bony prominences: technological concepts and clinical utilization *Wounds* **19**
[56] Gerhardt L C, Mattle N, Schrade G U, Spencer N D and Derler S 2008 Study of skin-fabric interactions of relevance to decubitus: friction and contact-pressure measurements *Skin Res. Technol.* **14** 77–88
[57] LeBlanc K and Baranoski S 2011 Skin tears: state of the science: consensus statements for the prevention, prediction, assessment, and treatment of skin tears *Adv. Skin Wound Care* **24** 2–15
[58] Lichterfeld-Kottner A, Hahnel E, Blume-Peytavi U and Kottner J 2017 Systematic mapping review about costs and economic evaluations of skin conditions and diseases in the aged *J. Tissue Viability* **26** 6–19
[59] Black J M, Cuddigan J E, Walko M A, Didier L A, Lander M J and Kelpe M R 2010 Medical device related pressure ulcers in hospitalized patients *Int. Wound J.* **7** 358–65
[60] Pailler-Mattei C, Debret R, Vargiolu R, Sommer P and Zahouani H 2013 *In vivo* skin biophysical behaviour and surface topography as a function of ageing *J. Mech. Behav. Biomed. Mater.* **28** 474–83
[61] Zahouani H, Boyer G, Pailler-Mattei C, Ben Tkaya M and Vargiolu R 2011 Effect of human ageing on skin rheology and tribology *Wear* **271** 2364–9